Two-Dimensional Combinatorial Screening Identifies Specific 6′-Acylated Kanamycin A− and 6′-Acylated Neamine−RNA Hairpin Interactions[†]

Olga Aminova,[‡] Dustin J. Paul,[‡] Jessica L. Childs-Disney,[§] and Matthew D. Disney*,[‡]

Department of Chemistry, University at Buffalo, The State University of New York, and the NYS Center of Excellence in Bioinformatics & Life Sciences, 657 Natural Sciences Complex, Buffalo, New York 14260, and Department of Chemistry & Biochemistry, Canisius College, 2001 Main Street, Buffalo, New York 14208

Received July 5, 2008; Revised Manuscript Received October 7, 2008

ABSTRACT: Herein, we report the RNA hairpin loops from a six-nucleotide hairpin library that bind 6′-acylated kanamycin A (**1**) and 6′-acylated neamine (**2**) identified by two-dimensional combinatorial screening (2DCS). Hairpins selected to bind **1** have K_d's ranging from 235 to 1035 nM, with an average K_d of 618 nM. For **2**, the selected hairpins bind with K_d's ranging from 135 to 2300 nM, with an average K_d of 1010 nM. The selected RNA hairpin−ligand interactions are also specific for the ligand that they were selected to bind compared with the other arrayed ligand. For example, the mixture of hairpins selected for **1** on average bind 33-fold more tightly to **1** than to **2**, while the mixtures of hairpins selected for **2** on average bind 11-fold more tightly to **2** than to **1**. Secondary structure prediction of the selected sequences was completed to determine the motifs that each ligand binds, and the hairpin loop preferences for **1** and **2** were computed. For **1**, the preferred hairpin loops contain an adenine separated by at least two nucleotides from a cytosine, for example, ANNCNN (two-tailed p-value = 0.0010) and ANNNCN (two-tailed p-value <0.0001). For **2**, the preferred hairpin loops contain both 5′GC and 5′CG steps (two-tailed p-value <0.0001). These results expand the information available on the RNA hairpin loops that bind small molecules and could prove useful for targeting RNA.

RNA plays important roles in biological systems beyond the transfer of genetic material. For example, microRNAs regulate RNA lifetime and contribute to cancer (*1*), riboswitches control gene expression by interacting with metabolites (*2*), and viral RNAs facilitate translation of viral proteins (*3*). The most studied RNA therapeutic target for small molecules is the bacterial ribosome; most antibacterials that target the ribosome form direct contacts with RNA (*4*). Other RNAs have been targeted with small molecules including HIV trans-activating response (TAR)[1] RNA (*5*) and rev-responsive element (RRE) RNA (*6*−*8*). Despite these studies, most RNA drug targets represent untapped potential.

One difficulty in exploiting other RNA targets for small molecule therapeutics is the relatively limited information available about the small RNA motifs that small molecules bind. What is known about RNA-binding ligands has come from studying smaller motifs or domains derived from RNA therapeutic targets. Such approaches have helped develop compounds to inhibit HIV infection by targeting TAR RNA (*7*), to inhibit bacterial growth by targeting the bacterial ribosome (*9, 10*), and to facilitate the elimination of plasmids that cause antibiotic resistance (*11, 12*).

To develop rational approaches to target RNA, information on the ligands that like to bind RNA and the RNA motifs that like to bind ligands is needed. The most commonly used methods to gather such information are systematic evolution of ligands by exponential enrichment (SELEX) and high-throughput screening. In SELEX, RNAs that bind a ligand of interest with high affinity (aptamers) are identified from an RNA library using multiple rounds of selection (*13*). Aptamers that bind to a ligand are typically large (∼15−20 nucleotides) and are therefore difficult to find in a biologically active RNA. In high-throughput screening, validated RNA drug targets (bacterial rRNA A-site or TAR RNA, for example) are screened for binding to a library of chemical ligands (*5, 14*). Screening of validated RNA targets, however, suffers from low hit rates. We previously described a method that merges RNA selection and ligand screening called two-dimensional combinatorial screening (2DCS) to identify RNA motif−ligand partners where the RNA motifs are small and likely to be found in a biologically important RNA (*15*). In 2DCS, a library of RNAs is screened against a library of

[†] This work was supported by funding from the University at Buffalo, the NYS Center of Excellence and Bioinformatics and Life Sciences, a New Investigator Award from the Camille and Henry Dreyfus Foundation, a Cottrell Scholar Award from the Research Corporation, a NYSTAR J. D. Watson Young Investigator Award, and the National Institutes of Health (Grant RO1-GM079235).

* To whom correspondence should be addressed. E-mail: mddisney@buffalo.edu. Phone: (716) 645-6800 ×2170. Fax: (716) 645-6963.

[‡] University at Buffalo and NYS Center of Excellence in Bioinformatics & Life Sciences.

[§] Canisius College.

[1] Abbreviations: A-site, aminoacyl-tRNA site; BSA, bovine serum albumin; DIS, dimerization initiation site; DMF, *N*,*N*-dimethylformamide; FITC, fluorescein isothiocyanate; HIV, human immunodeficiency virus; HPLC, high-performance liquid chromatography; MS, mass spectrometry; PCR, polymerase chain reaction; RRE, rev-response element; RT, reverse transcription; SELEX, systematic evolution of ligands by exponential enrichment; TAMRA, carboxytetramethylrhodamine; TAR, trans-activating response; TBTA, tris-(benzyltriazolylmethyl)amine; TEA, triethylamine; TLC, thin layer chromatography.

10.1021/bi8012615 CCC: $40.75
Published on Web 11/08/2008

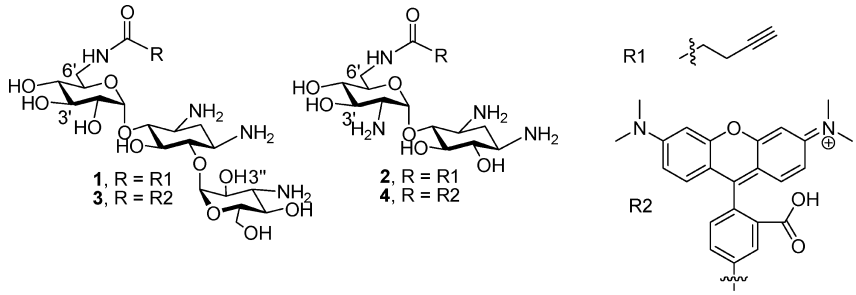

FIGURE 1: The structures of the ligands used to select and study RNA hairpin−ligand interactions. Structures **1** and **2** are derivatives of kanamycin A and neamine, respectively, that have been acylated at their 6′ positions with 5-hexynoate. These structures were immobilized onto azide-functionalized agarose via a Huisgen dipolar cycloaddition reaction. Structures **3** and **4** are 5-carboxytetramethylrhodamine (TAMRA)-labeled derivatives of **1** and **2**, respectively; they were used to study the affinities of the selected RNA hairpin−ligand interactions using a fluorescence-based assay.

ligands; the results help to define RNA motif−ligand partners. With the power of RNA structure prediction (*16*) and the availability of genomic sequence (*17, 18*), RNA motif−ligand partners that are the output of 2DCS could be mined for their presence in biologically important RNA using programs like *RNAmotif* (*19*).

Previously, 2DCS was used to identify the RNA internal loops that bind ligands (*15*). Herein, we have utilized 2DCS and a library of RNA hairpin loops to identify RNA hairpin loop−ligand interactions. The RNA library has six randomized positions in a hairpin pattern and therefore 4096 unique members. The ligands are 6′-acylated derivatives of the aminoglycosides kanamycin A (**1**) and neamine (**2**) (Figure 1). Our results show that the kanamycin A derivative prefers hairpins with an adenine (A) and a cytosine (C) separated by two or three nucleotides while the neamine derivative prefers hairpins with 5′GC and 5′CG steps. Comparison of the study reported herein to a previous study with an internal loop library (*20*) shows that the kanamycin A derivative binds more tightly to selected internal loops than to selected hairpin loops.

MATERIALS AND METHODS

General Array Construction and RNA Synthesis Methods. Oxidized agarose microarrays were functionalized with 3-azidopropylamine, and the aminoglycosides **1** and **2** were immobilized onto the array surface using a Huisgen dipolar cycloaddition reaction as described previously (*20, 21*). The six-nucleotide RNA hairpin library was transcribed using a synthetic DNA template purchased from Integrated DNA Technologies (Coralville, IA) in which the randomized nucleotides were custom-mixed to ensure equal representation of each nucleotide in the template. This DNA was PCR amplified to provide a double-stranded template with a T7 promoter and transcribed using a RNAMaxx transcription kit (Stratagene) per the manufacturer's protocol. After transcription, the product was purified using a denaturing 15% polyacrylamide gel and 5′-end labeled with [γ-^{32}P]ATP as described previously (*20*).

Competitor oligonucleotide **6** and oligonucleotide **9** (Figure 2) were purchased from Dharmacon and deprotected using the manufacturer's standard protocol. The deprotection solution was evaporated by vacuum concentration, and the oligonucleotides were used without further purification. Competitor oligonucleotides **7** and **8** were purchased from Integrated DNA Technologies and were used without further purification.

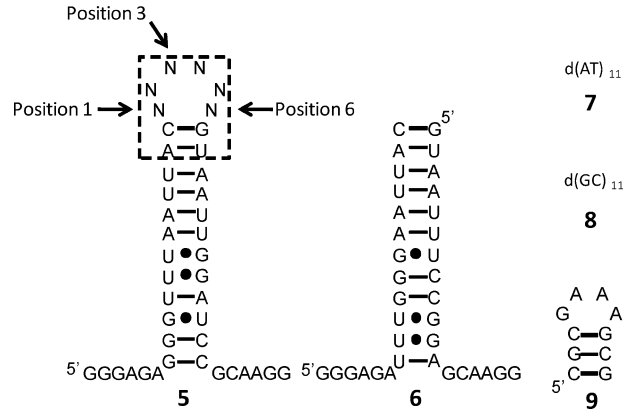

FIGURE 2: Oligonucleotides used to identify the RNA hairpin−ligand interactions via 2DCS. Oligonucleotide **5** is a RNA hairpin library with six randomized positions (N). The library has 4096 unique members. Oligonucleotides **6**−**8** were used at 10000 times the concentration of **1** in selection experiments to ensure that interactions occurred to loop nucleotides and not to the cassette. The oligonucleotides that comprise **6** are a mimic of the stem in **5**; the sequence was altered such that it does not compete for RT-PCR primers. Oligonucleotides **7** and **8** are DNA competitors. Oligonucleotide **9** was used to study the binding of 6′-acylated neamine to 5′CG and 5′GC steps.

*Hybridization of the Hairpin Library (**5**) and Competitor Oligonucleotides (**6**, **7**, and **8**) with Aminoglycoside Arrays.* Four tubes were prepared containing the following amounts of oligonucleotide(s) in 100 μL of hybridization buffer (HB, 8 mM $NaHPO_4$, 1 mM EDTA, 180 mM NaCl, pH 7.0): **5**, 5.5 pmol; **6**, 45.5 nmol; **7**, 45.5 nmol; and **8**, 45.5 nmol. The oligonucleotides were folded by incubation at 60 °C for 5 min and then slow cooling to room temperature. After reaching room temperature, the solutions were combined, and the final volume was adjusted to 500 μL with 1× HB. Prior to hybridization with the oligonucleotides, the array was prehybridized with 1× HB containing 0.1% BSA for 15 min at room temperature. The solution was removed from the array surface, and the solution containing all oligonucleotides was pipetted on the surface and spread evenly with a custom-cut piece of parafilm. The array was incubated for 20 min at room temperature. After hybridization, unbound RNA was washed from the surface using 1× HB, and the arrays were imaged as described previously (*20*). Positions on the agarose array where RNAs were captured were excised from the surface and amplified via RT-PCR as described previously (*21*). The RT-PCR product was then cloned into pGEM T Vector (Promega) according to the manufacturer's standard protocol. The ligation mixture was

used to transform *Escherichia coli* DH5-α competent cells. White colonies were used to inoculate 1 mL of Terrific Broth in a well of a deep-well 96-well plate. After the cultures reached an OD_{550} of ~4, the cultures were pelleted and sent to Functional Biosciences (Madison, WI) for sequencing.

Determination of Trends in Selected Hairpins. The secondary structures of the selected hairpins were predicted using the RNAstructure program (*16*). Trends in the sequence data for the hairpins selected for **1** and **2** were determined as described previously (*20*). In order to determine the number of hairpins in the library (**5**) that display the trend of interest, the program GNU Grep (version 2.5.1) was used (http://www.gnu.org/software/grep/grep.html). This freeware program searches for patterns and reports the number and sequence of library members that meet a given criterion.

*Transcription of RNA Pools and Individual Hairpins Selected To Bind **1** and **2**.* All RNAs were transcribed using an RNAMaxx transcription kit (Stratagene) using 5 μL of template from the RT-PCR reaction (hairpin mixtures) or from the PCR amplification reaction of the plasmid containing the individual hairpin loop of interest.

Affinity Measurements. Dissociation constants from direct assays were determined as described previously (*20*) using a Bio-Tek FLX-800 plate reader except 50 nM of **3** or **4** was used. The excitation and emission filters used were 530/25 and 590/35, respectively, and the sensitivity was set to 60. An approximately 35% decrease in fluorescence was observed. The resulting curves were fit to (*27*)

$$I = I_0 + 0.5\Delta\varepsilon[([FL]_0 + [RNA]_0 + K_t) - (([FL]_0 + [RNA]_0 + K_t)^2 - 4[FL]_0[RNA]_0)^{0.5})]$$

where I is the observed fluorescence intensity, I_0 is the fluorescence intensity in the absence of RNA, $\Delta\varepsilon$ is the difference between the fluorescence intensity in the absence of RNA and that in the presence of infinite RNA concentration with values usually ranging between 1.3×10^{-11} and 5.9×10^{-11} I M^{-1}, $[FL]_0$ is the total concentration of the fluorescently labeled aminoglycoside, $[RNA]_0$ is the total concentration of the selected hairpin loop(s) or control RNA, and K_t is the dissociation constant.

Competition assays were also completed as described previously using 1−1.25 μM RNA, 50 nM **3** or **4**, and increasing concentrations of competitor. The expected increase in fluorescence was observed, and the resulting curves were fit to (*23*)

$$\Theta = \frac{1}{2[FL]_0}\left[K_t + \frac{K_t}{K_d}[C_t]_0 + [RNA]_0 + [FL]_0 - \sqrt{\left(K_t + \frac{K_t}{K_d}[C_t]_0 + [RNA]_0 + [FL]_0\right)^2 - 4[FL]_0[RNA]_0}\right] + A$$

where Θ is the fraction of fluorescently labeled aminoglycoside bound, K_t is the dissociation constant determined for the hairpin of interest from a direct binding assay, K_d is the dissociation constant of the competing, unlabeled aminoglycoside, $[FL]_0$ is the total concentration of the fluorescently labeled aminoglycoside, $[C_t]_0$ is the total concentration of competing aminoglycoside, A is the amount of fluorescently labeled aminoglycoside that is bound at infinite concentration of unlabeled competitor with values ranging between 0 and 0.08, and $[RNA]_0$ is the total concentration of the hairpin of interest.

The two mixtures of hairpins selected to bind **1** and **2** were also tested for binding to 5-carboxytetramethlyrhodamine (TAMRA)-labeled propylamine, which serves as a negative control. No change in fluorescence was observed for either mixture up to 4 μM RNA concentration.

General Dye Conjugation and Other Synthetic Methods. Preparative TLCs were completed using Analtech preparative plates (20 cm × 20 cm, 500 μm thick). High-performance liquid chromatography (HPLC) separations were performed on a Waters 1525 binary pump system with an attached UV−vis detector, and absorbances at 220 and 254 nm were recorded. Purifications were completed using a Waters C8 preparative column (7 μm, 19 mm × 150 mm) with a flow rate of 5 mL/min and a solvent composition from 95% aqueous methanol with 0.1% trifluoroacetic acid (TFA) to 5% aqueous methanol with 0.1% TFA over 35 min. All compounds were >90% pure as determined by analytical HPLC. Mass spectra were collected on a Finnegan LC-MS using methanol as the running solvent. The mass range scanned was 200−2000 Da with the injector temperature set to either 190 or 250 °C. The tris-(benzyltriazolylmethyl)-amine (TBTA) catalyst (*24*) and 3-azidopropylamine (*25*) were synthesized as described previously. The aminoglycosides 1,3,3″-tri-*N*-(*tert*-butoxylcarbonyl)-kanamycin A, 1,3,2′-tri-*N*-(*tert*-butoxylcarbonyl)-neamine, 6′-*N*-5-hexynoate kanamycin A (**1**), and 6′-*N*-5-hexynoate neamine (**2**) were synthesized as described previously (*21*).

*Synthesis of TAMRA-Labeled Kanamycin A (**3**).* 1,3,3″-Tri-*N*-(*tert*-butoxylcarbonyl)-6′-*N*-5-hexynoate kanamycin A (1 mg, 1.2 μmol) was dissolved in 250 μL of *N*,*N*-dimethylformamide (DMF) with 2% triethylamine and reacted with 5-carboxytetramethylrhodamine (5-TAMRA) succinimidyl ester (1.2 μmol, Invitrogen) for 2 h at room temperature. The reaction was then lyophilized, resuspended in 100 μL of methanol and purified by preparative TLC using a solvent system of chloroform/methanol (10:4). The product (R_f, 0.1) was extracted from the silica gel with methanol and lyophilized to yield a dark pink powder. MS (ESI) expected 1197 (M^+); found 1197 (M^+, 100%). The material was then deprotected in 500 μL of TFA/dichloromethane (1:1) for 30 min at room temperature. The sample was lyophilized and purified by HPLC (t_r = 21.77 min). The product (0.6 mg, 55% overall) was obtained as a dark pink solid. MS (ESI) expected 897.3 (M^+); found 897 (M^+, 100%).

*Synthesis of TAMRA-Labeled Neamine (**4**).* 1,3,2′-Tri-*N*-(*tert*-butoxylcarbonyl)-neamine (2 mg, 2.7 μmol) was dissolved in 250 μL of DMF with 2% triethylamine and was reacted with 5-carboxytetramethylrhodamine succinimidyl ester (2.72 μmol) for 2 h at room temperature. The reaction was then lyophilized, resupsended in 100 μL of methanol, and purified by preparative TLC using a solvent system of chloroform/methanol (10:4). The product (R_f, 0.25) was extracted from the silica gel into methanol and lyophilized to a dark pink powder. MS (ESI) expected 1035 (M^+); found 1035 (M^+, 100%). The material was then deprotected in 500 μL of TFA/dichloromethane (1:1) for 30 min at room temperature. The sample was lyophilized and purified by HPLC (t_r = 21.50 min). The product (1.1 mg, 71% overall) was obtained as a dark pink solid. MS (ESI) expected 735 (M^+); found 735 (M^+, 100%).

Synthesis of TAMRA-Labeled Propylamine. A 2 μL aliquot of propylamine was dissolved in 250 μL of DMF with 2%

triethylamine and was reacted with 5-carboxytetramethylrhodamine succinimidyl ester (400 nmol) for 2 h at room temperature. The sample was lyophilized and purified by HPLC (t_r = 18.40 min). The product (200 nmol, 50% overall) was obtained as a dark pink solid. MS (ESI) expected 472 (M^+); found 472 (M^+, 100%).

RESULTS AND DISCUSSION

The aminoglycosides 6′-*N*-5-hexynoate kanamaycin A (**1**) and 6′-*N*-5-hexynoate neamine (**2**) were used as ligands to identify RNA hairpin−ligand interactions (Figure 1). These two aminoglycosides are acylated at their 6′ positions and mimic the product of modification by the 6′ aminoglycoside acetyltransferase family of resistance enzymes (*26*). Binding of kanamycin A to an oligonucleotide mimic of the bacterial rRNA A-site shows that acetylation at the 6′ position decreases aminoglycoside affinity to the A-site by 3 orders of magnitude (*27*). Prior to the result reported herein, no information was available on the RNA hairpin loops that bound **1**, while there was no information on any RNA structures that bound **2**. Previous studies have been completed to identify the internal loops that bind **1**, however (*20, 21*). These studies showed that **1** preferred internal loops displaying an adenine across from a cytosine and pyrimidine-rich loops.

The RNA hairpin library (**5**, Figure 2) contains six randomized positions, resulting in 4096 unique library members that display four- and six-nucleotide hairpins. Hairpins with four nucleotides result if a presumed base pair forms between positions 1 and 6. We chose to study small hairpins because they are common secondary structural elements (larger hairpins are less commonly found in biologically relevant RNAs) and often have functional importance. For example, hairpins serve as docking sites for proteins, are cellular localization elements (*28, 29*), form tertiary contacts within a RNA (*30*), and bind small molecules (*11, 12, 31*). Therefore, identifying the sequence and structural preferences of aminoglycosides for RNA hairpins is important.

To select RNA hairpin loop−ligand interactions via 2DCS, **1** and **2** were immobilized onto azide-functionalized agarose microarrays using a Huisgen dipolar cycloaddition reaction (*21, 24, 32*). Arrays were hybridized with ^{32}P-labeled **5** and competitor oligonucleotides **6**−**8** (Figure 2); **5** is the six-nucleotide hairpin library while **6** is a duplex mimic of the stem in **5**. Oligonucleotide **6** is used to select against sequence and structure elements that are common to all members of **5**. Oligonucleotides **7** and **8** are DNAs that ensure interactions are RNA-specific. Competitors were used in excess over the amount of ligand delivered to the array surface and the amount of **5** hybridized with the array (10000-fold excess each of **6**−**8**). After hybridization and washing away of unbound RNA, arrays were imaged to determine whether members of **5** bind **1** and **2** (Figure 3). A clear dose−response is observed for both aminoglycosides. Interestingly, comparison of these data with previously published data for **1** binding to a 3 × 3 nucleotide internal loop library (*21*) shows that a higher ligand loading is required to bind members of **5** (Figure 3). This may suggest that **1** binds internal loops with higher affinity than it does hairpin loops or that **1** binds more internal loops than hairpin loops. The binding data reported herein point to the former.

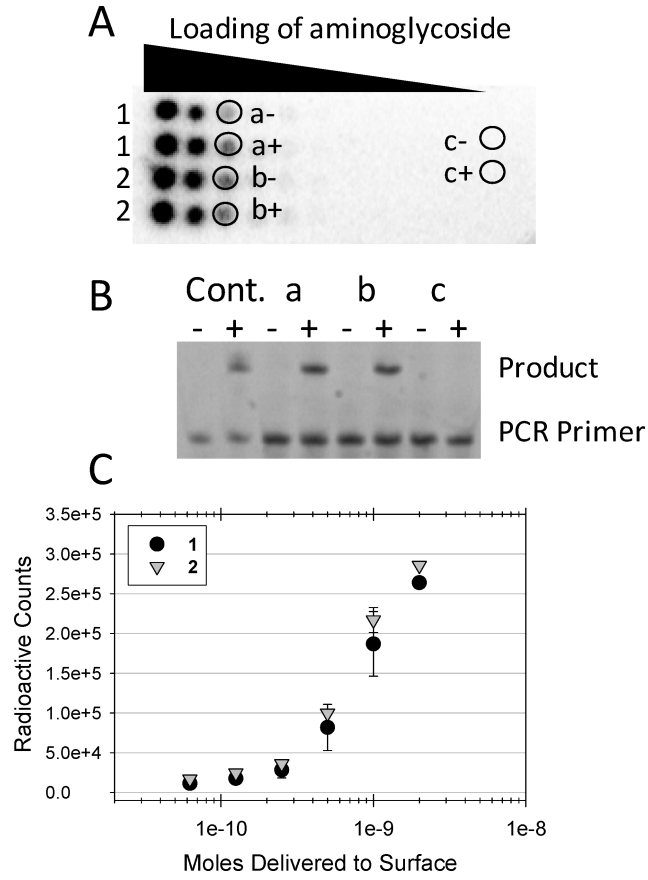

FIGURE 3: Selection of RNA hairpin−ligand interactions using array immobilized **1** and **2**: (A) An image of a microarray in which serially diluted concentrations (or loadings) of **1** and **2** (indicated to the left of the array) were anchored onto an azide−agarose array and hybridized with 5′-end ^{32}P-labeled **5** in the presence of competitor oligonucleotides **6**−**8**. Positions on the array from which RNA was excised are indicated with circles. Circles labeled "c+" and "c−" serve as background controls; no aminoglycoside was spotted in these positions. (B) An image of a gel for RT-PCR amplification of samples excised from the array in panel A; "−" indicates reactions completed in the absence of reverse transcriptase while "+" indicates reactions completed in the presence of reverse transcriptase. "Cont." indicates negative and positive controls in the absence or presence of reverse transcriptase. (C) A plot of the dose−response for the array shown in panel A.

Bound RNAs at the lowest ligand loading of **5** that was above background (where no aminoglycoside was spotted) were excised from the agarose array, RT-PCR amplified, cloned, and sequenced (Figure 3). The secondary structures of the sequences were predicted by free energy minimization (*21*) to determine the RNA motifs that bind each ligand (Figures 4 and 5). The motifs were then statistically analyzed to identify trends in the selected structure space to identify "consensus" RNA hairpins that bind **1** and **2**. Representative structures were then studied for binding to fluorescently labeled derivatives of **1** (compound **3**) and **2** (compound **4**) (Figure 1) to determine dissociation constants. In previous studies with internal loops, aminoglycoside derivatives were labeled by attaching 5-fluorescein isothiocyanate (5-FITC) to the product of 6′-*N*-5-hexynoate-modified aminoglycosides (**1** and **2**, for example) after reaction with 3-azidopropylamine via a Huisgen dipolar cylcoaddition (*32*). Titration of RNA hairpins into solutions of 5-FITC labeled **1** and **2**, however, showed little change in fluorescence (≤10%). Similar 5-carboxytetramethylrhodamine (TAMRA) derivatives were syn-

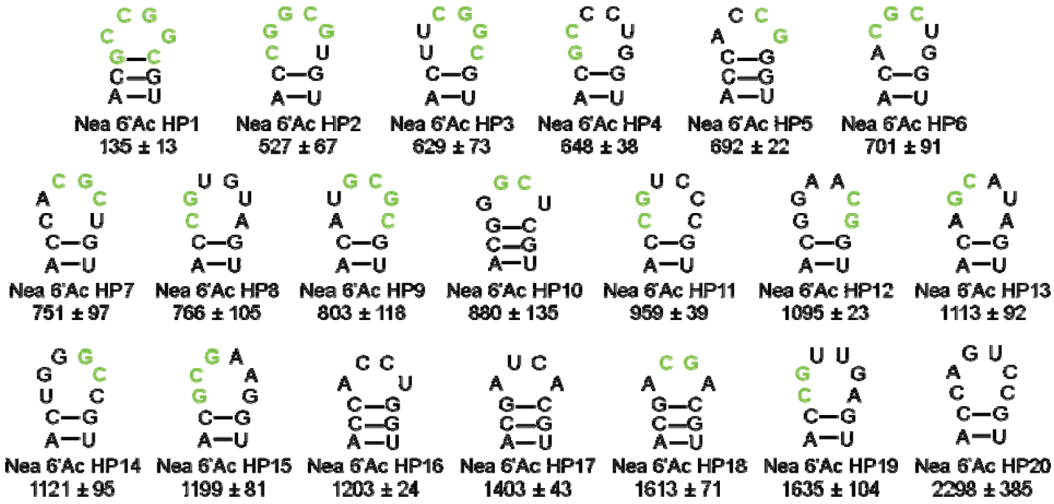

FIGURE 4: The secondary structures of a subset of the RNA hairpin loops that were selected to bind **2** (neamine derivative) and studied for binding **4.** The nucleotides shown are derived from the boxed region in **1**, and the affinities (nM) for **4** are shown below the hairpin structure. The green nucleotides highlight 5′GC and 5′CG steps.

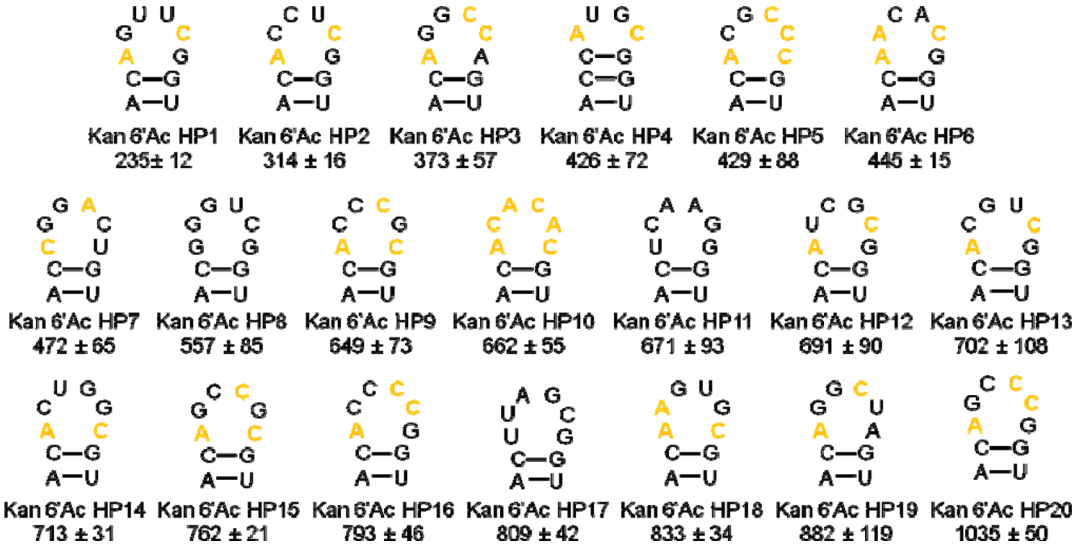

FIGURE 5: The secondary structures of a subset of the RNA hairpin loops that were selected to bind **1** (kanamycin A derivative) and studied for binding **3**. The nucleotides shown are derived from the boxed region in **1**, and the affinities (nM) for **3** are shown below the hairpin structure. The orange nucleotides highlight A's separated by at least two nucleotides from C's.

thesized and also gave small changes in fluorescence (≤10%) when titrated into solutions containing RNA hairpins. In contrast when the TAMRA dye was brought closer to the RNA by direct conjugation to the aminoglycoside's 6′-amine to yield compounds **3** and **4**, these compounds were responsive to RNA binding (change in fluorescence ~35%) and allowed accurate determination of binding constants.

RNA Hairpins That Bind to Neamine Derivative ***2.*** The hairpins that bind **2** were searched for commonalities (Figure 4). There was no preference for presumed four- or six-nucleotide hairpin loops, because they appear at the same approximate percentages in the selected structures and in the entire hairpin library. Nea 6′Ac HP15 appeared twice in the sequencing data. The only statistically significant trend in hairpins that bind **2** are loops that contain both 5′GC and 5′CG steps (two-tailed p-value <0.0001). Dissociation constants were determined for a subset of selected hairpins that fall into four categories—hairpins that have both 5′GC and 5′CG steps (average K_d of 678 nM), hairpins that have 5′GC steps (average K_d of 941 nM), hairpins that have 5′CG steps (average K_d of 1127 nM), and hairpins that have no 5′GC or 5′CG steps (average K_d of 1635 nM) (Figure 4).

Inspection of the hairpin loops in Figure 4 shows that a few hairpins, like Nea 6′Ac HP1, have the potential to form kissing complexes or fully paired duplexes. It should be noted that kissing hairpins are stabilized by divalent metal ions because these complexes bring several phosphates close together (*33*); however, Mg^{2+} was not present in the hybridization buffer used herein. In order to address the secondary structure formed by the hairpins, a subset was studied by native gel electrophoresis and Nea 6′Ac HP1 was studied by native gel, enzymatic mapping, and optical melting. All three methods confirm that hairpins as depicted in Figure 4 are forming; only a single band for all RNAs is observed in native gels with similar mobility as the corresponding GAAA hairpin and **5**. Furthermore, native gel electrophoresis in the presence of **4** did not induce the formation of kissing hairpins. The hairpin loop guanines are accessible to T1 nuclease cleavage indicating that they are single-stranded. There is no concentration dependence on

Table 1: The Selectivities of the Hairpins Selected To Bind to **1** or **2**[a]

	direct assays			competition assays		
	K_d for selected aminoglycoside (nM)	K_d for other aminoglycoside (nM)	selectivity	K_d for selected aminoglycoside (nM)	K_d for other aminoglycoside (nM)	selectivity
Kan HP mixture[b]	680 ± 11			164 ± 22	5430 ± 396	33
Kan HP1	235 ± 12	~4000	17		<25000	
Kan HP2	314 ± 16	2800 ± 146	9		<25000	
Kan HP3	373 ± 57	1800 ± 26	5		<25000	
Kan HP5	429 ± 88	2200 ± 303	5		<25000	
Nea HP mixture[b]	1150 ± 166			275 ± 53	~3000	~11
Nea HP1	135 ± 13	~3000	~22	89 ± 22	~5000	~55
Nea HP3	629 ± 73	~5000	~7	115 ± 11	~4000	~35
Nea HP5	692 ± 22	~3000	~4	94 ± 14	~3000	~30
Nea HP7	751 ± 97	2000 ± 272	3	91 ± 16	~7000	~70

[a] Selectivities were determined by dividing the K_d determined for the other aminoglycoside by the K_d determined for the selected aminoglycoside. [b] These RNAs are the mixtures of hairpins that were harvested via 2DCS for binding **1** or **2**.

the melting temperature in optical melting experiments, and there is only a single transition at all concentrations tested, up to 6 μM. Please see the Supporting Information for experimental procedures and data from these experiments.

The affinity of the mixture of hairpins selected to bind **2** was then determined using **4**. The mixture selected to bind **2** binds to **4** with a dissociation constant of 1150 ± 166 nM. A competition assay with **2** was used to determine the effect that dye conjugation has on affinity. This experiment revealed that the fluorophore decreases affinity by about 4-fold giving a dissociation constant of 275 ± 53 nM; such effects have been observed previously (*22, 34*). The selectivity of the mixture of hairpins selected to bind **2** was also studied using a competition assay with **1**. The hairpins that bind **2** are about 11-fold selective as they bind **1** with a K_d of ~3000 nM. In order to determine whether the hairpins bind to the dye alone, the binding of the mixture of hairpins to TAMRA-propylamine was studied. No change in fluorescence was observed up to 4 μM RNA concentration, indicating that the dye does not bind RNA unless conjugated to the aminoglycoside.

Surprisingly, **5** (the entire hairpin library) binds to **2** with a K_d of 4200 ± 283 nM, or only about a 4-fold decrease in affinity compared with the selected hairpins. Since a statistically significant trend was found for the loops selected to bind **2**, these data were surprising. Careful inspection of the stem in **5** revealed a 5′CG and a 5′GC at the helix terminus and in the unpaired region, which are also present in **6**. We therefore also studied the binding of **4** to **6**, a mimic of the stem in **5** that contains both types of steps, **8**, $d(GC)_{11}$, and **9**, a small hairpin that contains 5′CG and 5′GC steps in the stem. **6** binds to **4** with a dissociation constant of 2200 ± 177 nM while the dissociation constant for **8** is 2300 ± 142, which likely reflect nonspecific binding. In contrast, **9** has a dissociation constant of 500 ± 40 nM. This suggests that **2** prefers 5′GC and 5′CG steps in or adjacent to RNA hairpin loops more than 5′GC and 5′CG steps distant from a hairpin loop.

The range of affinities for the hairpins selected to bind **2** (135−2298 nM, Figure 4) is consistent with the dissociation constant for the mixture of hairpins (1150 ± 166). The average dissociation constant for hairpins containing both 5′GC and 5′CG steps is 678 nM. The hairpins containing only 5′GC steps bind with the second highest affinity with an average K_d of 941 nM. Hairpins with only 5′CG steps or with neither 5′GC nor 5′CG steps bind more weakly with average dissociation constants of 1127 and 1635 nM, respectively. The dissociation constant for hairpins containing neither 5′GC nor 5′CG steps is similar to the K_d for **6**, a mimic of the stems (2200 nM).

The highest affinity hairpin for **2** is a 4-nucleotide loop closed by a GC base pair (Nea 6′Ac HP1, Figure 4). The hairpin contains multiple 5′GC and 5′CG steps and binds **2** and **4** with dissociation constants of 89 ± 22 and 135 ± 13 nM, respectively. A direct assay with **3** and competition assay with **1** were used to determine the selectivity of this loop. Nea 6′Ac HP1 prefers **4** ~22-fold over **3** and **2** ~55-fold over **1** (K_d is ~5000 nM). Three other hairpins were also studied for selectivities for **2** over **1**: Nea 6′Ac HP3 (115 ± 11 nM), Nea 6′Ac HP5 (94 ± 14 nM), and Nea 6′Ac HP7 (91 ± 16 nM) have selectivities of ~35, ~30, and ~70, respectively (Table 1). (Selectivies for **4** over **3** are ~7-, ~4-, and 3-fold, respectively, for Nea 6′Ac HP3, Nea 6′AC HP5, and Nea 6′Ac HP7.) Despite the weak binding of **4** to the stem region, high affinity, selective hairpin loop−**2** interactions were identified from 2DCS. This is likely due to the presence of competitor oligonucleotides in a large excess of **5** (10000-fold each) and in excess to the amount of ligand arrayed on the surface.

The cassette in which Nea 6′Ac HP1 was displayed was altered to determine whether cassette nucleotides are important for binding. One cassette contained all GC base pairs, while the other contained all AU base pairs (Figure 6). Not surprisingly, the binding of **4** to Nea 6′Ac HP1 when displayed in the GC cassette was only approximately 1.5-fold tighter than the binding of **4** to the GC cassette with a GAAA tetraloop (367 ± 11 nM and 555 ± 10 nM, respectively), consistent with our other observations. Binding of **4** to Nea 6′Ac HP1 when displayed in **5** and the AU cassette was similar, 135 ± 13 and 152 ± 21 nM, respectively. No change in fluorescence was observed up to 4 μM of the AU cassette. These data also point to 6′-acylated neamine preferring RNA hairpins with 5′GC and 5′CG steps.

RNA Hairpins That Bind the Kanamycin A Derivative, ***1.*** Sequence trends were identified in the hairpins selected to bind **1** (Figure 5). As for the case of **2**, **1** has no preference for four- or six-nucleotide hairpins. Two hairpins appeared twice in the sequencing data, Kan 6′Ac HP9 and Kan 6′Ac HP18. Kan 6′Ac HP17 has the same loop nucleotides as Kan 6′ Ac HP1 though the order is different. Many loops have A in the first position (41.8%, two-tailed p-value = 0.0113), the only position where a clear nucleotide preference was observed for either aminoglycoside. The most statistically

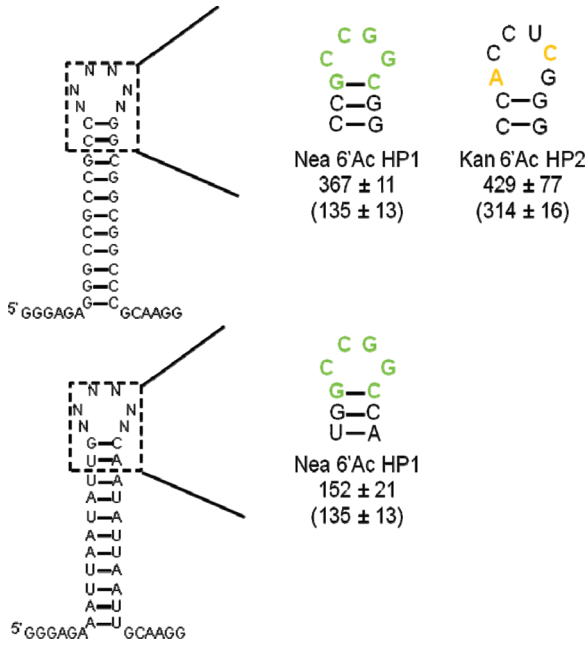

FIGURE 6: The GC and AU cassettes into which Nea 6′Ac HP1 and Kan 6′Ac HP2 were inserted. The dissociation constants (nM) in the corresponding cassette are given below the secondary structure of the hairpin. The dissociation constants (nM) in the original cassette (**5**) are shown in parentheses. The dissociation constant for **4** binding to the GC and AU cassettes are 555 ± 10 nM and >4000 nM, respectively. The dissociation constant for **3** binding to the GC cassette is ~4 μM. The orange and green nucleotides indicate statistically significant trends identified from sequencing data.

significant trend is A in position 1, C in position 5, and G in position 6. Seven out of 43 loops display this pattern giving a two-tailed *p*-value of <0.0001. Only 64 of 4096 members of the library (**5**) display this pattern. A more generic trend is A across from C. There are 1909 loops in the library that have the following trend •*A•*C•*, where the "•" indicates any nucleotide and the "*" indicates there can be any number of nucleotides before the A, any number of nucleotides separating the A and the C and any number of nucleotides after the C. In our selection, 29/43 loops displayed this trend giving a two-tailed *p*-value of 0.0065.

A more specific trend with A across from C is A in position 1 and C in position 5. There are 256 loops in the library with this trend (6.25%) compared with 11/43 loops from our selection (25.6%), corresponding to a two-tailed *p*-value of <0.0001. If A is not constrained to position 1 but must be separated by three nucleotides from a C, then 13 out of 43 hairpins fall into this category (two-tailed *p*-value = 0.0003). There are also many loops that have A in position 1 and C in position 4 (two-tailed *p*-value = 0.0010). The number of hairpins in **5** that have A in position 1 and C in position 4 or 5 is 448. In our selection, 15/43 hairpins display either trend, yielding a two-tailed *p*-value of <0.0001.

The affinity of the mixture of hairpins selected to bind **1** was determined using a fluorescence-based assay with **3**. The mixture binds **3** with a dissociation constant of 680 ± 11 nM. In constrast, **5** (the entire hairpin library) binds **1** with a dissociation constant of ~8 μM. In order to determine the effect of dye conjugation on affinity, a competition experiment with **1** was completed. The resulting K_d of 164 ± 22 nM indicates that the fluorophore interferes with binding to a similar extent that **4** did with the hairpins selected to bind **2**; in both cases, there is a 4-fold energetic penalty. The same competition experiment was also used to determine the affinity of **2** for the hairpins selected to bind **1**. These hairpins bind **2** much more weakly with a dissociation constant of 5430 ± 396 nM. Therefore, the mixture of hairpins is on average 33-fold selective for **1** over **2**. When the dissociation constants of **1** to internal loops and hairpin loops are compared, **1** prefers internal loops to hairpin loops by about 10-fold even though there are similarities in sequence (*20, 21*). Analogous to the results with the mixture of **2**-selected hairpins and TAMRA-propylamine, no change in fluorescence of TAMRA-propylamine was observed up to 4 μM of **1**-selected hairpins.

The dissociation constants for the individual hairpin loops selected to bind **1** (Figure 5) range from 235−1035 nM (the average K_d is 618 nM) and are reflective of the dissociation constant of the mixture of hairpins selected to bind **1** (680 nM). Interestingly, the two highest affinity hairpins (Kan 6′Ac HP1 and Kan 6′Ac HP2) share common features with high-affinity internal loops selected to bind **1** (*32*). Both contain adenine across from cytosine and pyrimidines in the loop; adenine and cytosine can form protonated base pairs. In order to determine the effect of pH on binding **1**, the dissociation constants for three hairpins were determined at pH 5.9. Kan 6′Ac HP1 has a dissociation constant of 285 ± 21 nM at pH 5.9 compared with 235 ± 12 nM at pH 7.0. For Kan 6′Ac HP2, these values are 545 ± 20 and 314 ± 16 nM at pH 5.9 and pH 7.0, respectively, while for Kan 6′Ac HP3, the dissociation constants are 488 ± 88 nM at pH 5.9 and 373 ± 57 nM at pH 7.0. The interpretation of these results is not straightforward, however, since the $3NH_2$ of kanamycin A has a pK_a of 6.2 (*35, 36*). Thus, it is difficult to determine whether the binding affinity is unaffected (Kan 6′Ac HP1 and HP3) or slightly weaker (Kan 6′Ac HP2) due to changes or lack thereof in the RNA structure or the different protonation state of **3**.

The selectivities of four hairpins selected to bind **1** (Kan 6′Ac HP1, Kan 6′Ac HP2, Kan 6′Ac HP3, and Kan 6′Ac HP5, Figure 5) were studied using direct and competition assays with **4** and **2**, respectively (Table 1). As expected, the four kanamycin hairpins bind more weakly to **4** in direct assays than **3**, with dissociation constants of ~4000, 2800 ± 146, 1800 ± 26, and 2200 ± 303 nM, respectively. Based on these values, the selectivities of the four kanamycin hairpins range from 5- to 17-fold, which is less than the 33-fold determined for the mixture of hairpins using a competition assay with **2**. Since the dissociation constants determined for the **1**-selected hairpins and **4** from direct assays are similar to the dissociation constants for the entire hairpin library (**5**, 4200 nM) and a mimic of the stem in **5** (**6**, 2200 nM), it is likely that **4** is binding to the **1**-selected hairpins in the same way, either nonspecifically or to the 5′GC and 5′CG steps at the bottom of the stem. To confirm that **2** is binding to a different site than **1**, competition assays were completed. Interestingly, fluorescence was not rescued up to 25 μM of **2** (500-fold excess of **2** over **3** (fluorescently labeled kanamycin derivative) and 25-fold excess over the RNA concentration). Taken together, this suggests **1** is binding to the hairpin loop while **2** is binding elsewhere.

To determine whether cassette nucleotides contribute to binding affinity, the cassette in which Kan 6′Ac HP2 was

displayed was altered. All pairs in the stem were mutated to GC (Figure 6). When displayed in **5**, the K_d for Kan 6′Ac HP2 is 314 ± 16 nM, while the K_d in the GC cassette is 429 ± 77 nM. (The dissociation constant for the cassette with all GC pairs in which the random region is altered to 5′CGAAAG is ~4 μM.) Thus, cassette nucleotides do not contribute significantly to binding since the dissociation constants are similar as was also observed in previous studies with an internal loop library (*15, 20*).

Comparison to Previous Aminoglycoside−RNA Studies. Many groups have studied aminoglycoside−RNA interactions using defined RNA targets including the bacterial A-site (*37*−*41*), HIV TAR RNA (*7, 42*), HIV RRE RNA (*8, 43*−*45*), group I introns (*46*−*50*), the hammerhead ribozyme (*51*), the hepatitis delta virus (*52*), and RNase P RNAs (*53, 54*). In each case, aminoglycosides inhibited the normal function of the RNA, and the binding site was identified. Despite these investigations, sequence preferences for aminoglycosides could not be identified; rather it was determined that aminoglycosides bind to pockets in tertiary structure or metal ion binding sites. In order to identify RNA sequence or structural preferences for aminoglycosides, other groups have used SELEX (*34, 55*−*58*).

We previously reported the selection of members of a 3 × 3 nucleotide internal loop library that bind a different neamine derivative (5-*O*-(2-azidoethyl)neamine). It was determined from that study that neamine binds a variety of internal loops, and no sequence or structural preferences were identified (*15*). In contrast, 2DCS identified "consensus" RNA hairpin loops that bind 6′-acylated neamine. This may be due to the lower number of hairpin loops that 6′-acylated neamine binds relative to the number of internal loops that bind 5-*O*-(2-azidoethyl)neamine. Acylation of the 6′NH_2 may minimize the RNA binding promiscuity of neamine by removing the most basic nitrogen.

The binding of neamine to validated drug targets has also been studied. For example, a crystal structure of an oligonucleotide mimic of the bacterial rRNA A-site was solved and compared with complexes with other aminoglycosides (*59*). (The oligonucleotide mimic used in these studies contains two copies of the A-site.) The A-site−aminoglycoside complexes show specific binding modes with gentamicin, neomycin B, and lividomycin A, and specific and nonspecific binding modes with kanamycin and ribostamycin. The complex formed with neamine, however, was slightly different. Only one of the two binding sites is occupied, and in the occupied site, the UU base pair does not form; instead U_{1406} bulges out of the duplex. Interestingly, the bound neamine hydrogen bonds to G_{1494} (which is based paired to C_{1407}; the base pair closes an all-adenine 1 × 2 nucleotide loop), the G_{1405}−C_{1496} base pair, and G_{1491} (which is base paired to C_{1409}). It also stacks on the C_{1409}−G_{1491} base pair that closes one side of the 1 × 2 nucleotide loop.

Neamine and neamine dimers have also been studied for binding to HIV RNA targets including RRE RNA (*8, 44, 45*) and the dimerization initiation site (DIS) RNA (*60, 61*). Interestingly, both RNA−ligand binding sites contain 5′GC and 5′CG steps. Previous studies identified that neomycin B binds to HIV RRE RNA, mapping the interactions to a 2 × 3 nucleotide internal loop and surrounding base pairs (*44, 45*). Based on these studies, a library of peptido-aminoglycosides was synthesized with a neamine core, some of which are better inhibitors of the REV−RRE complex than neomycin B (*8*).

The DIS RNA forms a kissing hairpin that is essential for replication; inhibition of the RNA complex therefore might serve as a therapeutic for HIV. There are variants of the DIS hairpin, each containing at least one 5′GC step. In fact, one variant's hairpin sequence is 5′GAAGCGCGCAC. It has been shown that neamine is a better inhibitor of kissing hairpin formation than neomycin, that affinity can be increased using neamine dimers, and that tobramycin binds unspecifically and with lower affinity (tobramycin is closely related to kanamycin) (*60, 61*). A crystal structure of neamine dimers bound to DIS kissing hairpins has been reported. Interestingly, when bound, the neamine dimers sit between GC base pairs formed when dimerization occurs, reminiscent of the neamine−A-site complex (*61*). These results coupled with our studies suggest that neamine prefers to bind RNA targets with several 5′GC steps in a row. Such information is critical to identify better RNA drug targets for aminoglycosides.

The hairpin loops that were selected to bind **1** share similar features with previous selections for kanamycin derivatives completed in our laboratory and others. In three internal loop selections with kanamycin derivatives, commonalities between selected loops were identified (*15, 20*). These include loops that display an adenine across from a cytosine and pyrimidine-rich internal loops. Interestingly, these are also features that were identified in our hairpins though they bind approximately 10-fold more weakly. In each case, only one round of selection was required to identify loop preferences for kanamycin derivatives. An aptamer for kanamycin B with picomolar affinity was selected by Kwon et al. after 12 rounds of selection (*56*). The aptamer contained a 1 × 1 nucleotide A−C internal loop closed with one GU and one AU base pair. The hairpin loop that capped the stem containing the internal loop also had an adenine and a cytosine, CCAUGG. Kan 6′Ac HP5 (Figure 5) has the same nucleotides as this loop but not the same sequence. Another kanamycin apatmer was reported by Werstuck and Green in which the hairpin loop also contains a cytosine across from an adenine (*55*). It will therefore be interesting to determine whether both AC-containing internal and hairpin loops present functional groups in a similar manner to interact with **1** and whether these loops indeed form protonated AC pairs.

SUMMARY

Herein, we have described the hairpin loops preferred by 6′-acylated kanamycin and neamine derivatives identified by 2DCS. Sequence preferences were found for both aminoglycosides: hairpins displaying adenine across from cytosine for kanamycin and hairpins with 5′GC and 5′CG steps for neamine. The hairpins bind with nanomolar affinities and are selective for the aminoglycoside for which they were selected. This information may have applications in facilitating the rational and modular design of small molecule targeting RNA; genomic RNA structures can be mined for targets that contain motifs identified in this study and others.

ACKNOWLEDGMENT

We thank anonymous reviewers for helpful suggestions and Profs. Dan Gaile and Lara Sucheston in the Dept. of

Biostatistics at the University at Buffalo and the New York State Center of Excellence in Bioinformatics and Life Sciences for assistance in identifying trends in sequence data. We also thank Mark J. Morris for initial experiments and David Strite and Lisa Strite for assistance with the GNU Grep program and for helpful discussions.

SUPPORTING INFORMATION AVAILABLE

Native gel electrophoresis experiments to determine whether Nea 6′Ac HP1, HP2, and HP9 dimerize or form duplexes instead of hairpins, enzymatic mapping experiments of Nea 6′Ac HP1 to confirm hairpin formation, optical melting experiments of Nea 6′Ac HP1 to confirm hairpin formation, sequences of all loops selected to bind Kan 6′Ac, and sequences of all loops selected to bind Nea 6′Ac. This material is available free of charge via the Internet at http://pubs.acs.org.

REFERENCES

1. Calin, G. A., and Croce, C. M. (2006) MicroRNAs and chromosomal abnormalities in cancer cells. *Oncogene 25*, 6202–6210.
2. Nahvi, A., Sudarsan, N., Ebert, M. S., Zou, X., Brown, K. L., and Breaker, R. R. (2002) Genetic control by a metabolite binding mRNA. *Chem. Biol. 9*, 1043–1049.
3. Ji, H., Fraser, C. S., Yu, Y., Leary, J., and Doudna, J. A. (2004) Coordinated assembly of human translation initiation complexes by the hepatitis C virus internal ribosome entry site RNA. *Proc. Natl. Acad. Sci. U.S.A. 101*, 16990–16995.
4. Tenson, T., and Mankin, A. (2006) Antibiotics and the ribosome. *Mol. Microbiol. 59*, 1664–1677.
5. Mei, H. Y., Mack, D. P., Galan, A. A., Halim, N. S., Heldsinger, A., Loo, J. A., Moreland, D. W., Sannes-Lowery, K. A., Sharmeen, L., Truong, H. N., and Czarnik, A. W. (1997) Discovery of selective, small-molecule inhibitors of RNA complexes--I. The Tat protein/TAR RNA complexes required for HIV-1 transcription. *Bioorg. Med. Chem. 5*, 1173–1184.
6. Hendrix, M., Priestley, E. S., Joyce, G. F., and Wong, C. H. (1997) Direct observation of aminoglycoside-RNA interactions by surface plasmon resonance. *J. Am. Chem. Soc. 119*, 3641–3648.
7. Baker, T. J., Luedtke, N. W., Tor, Y., and Goodman, M. (2000) Synthesis and anti-HIV activity of guanidinoglycosides. *J. Org. Chem. 65*, 9054–9058.
8. Park, W. K. C., Auer, M., Jaksche, H., and Wong, C. H. (1996) Rapid combinatorial synthesis of aminoglycoside antibiotic mimetics: Use of a polyethylene glycol-linked amine and a neamine-derived aldehyde in multiple component condensation as a strategy for the discovery of new inhibitors of the HIV RNA Rev responsive element. *J. Am. Chem. Soc. 118*, 10150–10155.
9. Greenberg, W. A., Priestley, E. S., Sears, P. S., Alper, P. B., Rosenbohm, C., Hendrix, M., Hung, S. C., and Wong, C. H. (1999) Design and synthesis of new aminoglycoside antibiotics containing neamine as an optimal core structure: Correlation of antibiotic activity with in vitro inhibition of translation. *J. Am. Chem. Soc. 121*, 6527–6541.
10. Kaul, M., Barbieri, C. M., and Pilch, D. S. (2006) Aminoglycoside-induced reduction in nucleotide mobility at the ribosomal RNA A-site as a potentially key determinant of antibacterial activity. *J. Am. Chem. Soc. 128*, 1261–1271.
11. Thomas, J. R., DeNap, J. C., Wong, M. L., and Hergenrother, P. J. (2005) The relationship between aminoglycosides' RNA binding proclivity and their antiplasmid effect on an IncB plasmid. *Biochemistry 44*, 6800–6808.
12. Denap, J. C., Thomas, J. R., Musk, D. J., and Hergenrother, P. J. (2004) Combating drug-resistant bacteria: small molecule mimics of plasmid incompatibility as antiplasmid compounds. *J. Am. Chem. Soc. 126*, 15402–15404.
13. Osborne, S. E., and Ellington, A. D. (1997) Nucleic acid selection and the challenge of combinatorial chemistry. *Chem. Rev. 97*, 349–370.
14. Mei, H. Y., Cui, M., Lemrow, S. M., and Czarnik, A. W. (1997) Discovery of selective, small-molecule inhibitors of RNA complexes--II. Self-splicing group I intron ribozyme. *Bioorg. Med. Chem. 5*, 1185–1195.
15. Disney, M. D., Labuda, L. P., Paul, D. J., Poplawski, S. G., Pushechnikov, A., Tran, T., Velagapudi, S. P., Wu, M., and Childs-Disney, J. L. (2008) Two-dimensional combinatorial screening identifies specific aminoglycoside-RNA internal loop partners. *J. Am. Chem. Soc. 130*, 11185–11194.
16. Mathews, D. H., Disney, M. D., Childs, J. L., Schroeder, S. J., Zuker, M., and Turner, D. H. (2004) Incorporating chemical modification constraints into a dynamic programming algorithm for prediction of RNA secondary structure. *Proc. Natl. Acad. Sci. U.S.A. 101*, 7287–7292.
17. Venter, J. C., et al. (2001) The sequence of the human genome. *Science 291*, 1304–1351.
18. Lander, E. S., et al. (2001) Initial sequencing and analysis of the human genome. *Nature 409*, 860–921.
19. Macke, T. J., Ecker, D. J., Gutell, R. R., Gautheret, D., Case, D. A., and Sampath, R. (2001) RNAMotif, an RNA secondary structure definition and search algorithm. *Nucleic Acids Res. 29*, 4724–4735.
20. Childs-Disney, J. L., Wu, M., Pushechnikov, A., Aminova, O., and Disney, M. D. (2007) A small molecule microarray platform to select RNA internal loop-ligand interactions. *ACS Chem. Biol. 2*, 745–754.
21. Disney, M. D., and Childs-Disney, J. L. (2007) Using selection to identify and chemical microarray to study the RNA internal loops recognized by 6′-*N*-acylated kanamycin A. *ChemBioChem 8*, 649–656.
22. Wang, Y., and Rando, R. R. (1995) Specific binding of aminoglycoside antibiotics to RNA. *Chem. Biol. 2*, 281–290.
23. Disney, M. D., Haidaris, C. G., and Turner, D. H. (2001) Recognition elements for 5′ exon substrate binding to the *Candida albicans* group I intron. *Biochemistry 40*, 6507–6519.
24. Chan, T. R., Hilgraf, R., Sharpless, K. B., and Fokin, V. V. (2004) Polytriazoles as copper(I)-stabilizing ligands in catalysis. *Org. Lett. 6*, 2853–2855.
25. Carboni, B., Benalil, A., and Vaultier, M. (1993) Aliphatic amino azides as key building-blocks for efficient polyamine syntheses. *J. Org. Chem. 58*, 3736–3741.
26. Magnet, S., and Blanchard, J. S. (2005) Molecular insights into aminoglycoside action and resistance. *Chem. Rev. 105*, 477–498.
27. Llano-Sotelo, B., Azucena, E. F., Jr., Kotra, L. P., Mobashery, S., and Chow, C. S. (2002) Aminoglycosides modified by resistance enzymes display diminished binding to the bacterial ribosomal aminoacyl-tRNA site. *Chem. Biol. 9*, 455–463.
28. Johnstone, O., and Lasko, P. (2001) Translational regulation and RNA localization in *Drosophila* oocytes and embryos. *Annu. Rev. Genet. 35*, 365–406.
29. Van De Bor, V., Hartswood, E., Jones, C., Finnegan, D., and Davis, I. (2005) *gurken* and the *I* factor retrotransposon RNAs share common localization signals and machinery. *Dev. Cell 9*, 51–62.
30. Cate, J. H., Gooding, A. R., Podell, E., Zhou, K., Golden, B. L., Kundrot, C. E., Cech, T. R., and Doudna, J. A. (1996) Crystal structure of a group I ribozyme domain: Principles of RNA packing. *Science 273*, 1678–1685.
31. Moehle, K., Athanassiou, Z., Patora, K., Davidson, A., Varani, G., and Robinson, J. A. (2007) Design of β-hairpin peptidomimetics that inhibit binding of α-helical HIV-1 rev protein to the rev response element RNA. *Angew. Chem., Int. Ed. 24*, 24.
32. Kolb, H. C., Finn, M. G., and Sharpless, K. B. (2001) Click chemistry: Diverse chemical function from a few good reactions. *Angew. Chem., Int. Ed. 40*, 2021.
33. Tinoco, I., Jr., and Bustamante, C. (1999) How RNA folds. *J. Mol. Biol. 293*, 271–281.
34. Wang, Y., Killian, J., Hamasaki, K., and Rando, R. R. (1996) RNA molecules that specifically and stoichiometrically bind aminoglycoside antibiotics with high affinities. *Biochemistry 35*, 12338–12346.
35. Kaul, M., Barbieri, C. M., Srinivasan, A. R., and Pilch, D. S. (2007) Molecular determinants of antibiotic recognition and resistance by aminoglycoside phosphotransferase (3′)-IIIa: a calorimetric and mutational analysis. *J. Mol. Biol. 369*, 142–156.
36. Walter, F., Vicens, Q., and Westhof, E. (1999) Aminoglycoside-RNA interactions. *Curr. Opin. Chem. Biol. 3*, 694–704.
37. Recht, M. I., Fourmy, D., Blanchard, S. C., Dahlquist, K. D., and Puglisi, J. D. (1996) RNA sequence determinants for aminoglycoside binding to an A-site rRNA model oligonucleotide. *J. Mol. Biol. 262*, 421–436.
38. Ryu, D. H., and Rando, R. R. (2001) Aminoglycoside binding to human and bacterial A-site rRNA decoding region constructs. *Bioorg. Med. Chem. 9*, 2601–2608.

39. Kaul, M., and Pilch, D. S. (2002) Thermodynamics of aminoglycoside−rRNA recognition: The binding of neomycin-class aminoglycosides to the A-site of 16S rRNA. *Biochemistry 41*, 7695–7706.
40. Kaul, M., Barbieri, C. M., Kerrigan, J. E., and Pilch, D. S. (2003) Coupling of drug protonation to the specific binding of aminoglycosides to the A-site of 16S rRNA: Elucidation of the number of drug amino groups involved and their identities. *J. Mol. Biol. 326*, 1373–1387.
41. Kaul, M., Barbieri, C. M., and Pilch, D. S. (2005) Defining the basis for the specificity of aminoglycoside-rRNA recognition: A comparative study of drug binding to the A-sites of *Escherichia coli* and human rRNA. *J. Mol. Biol. 346*, 119–134.
42. Krebs, A., Ludwig, V., Boden, O., and Gobel, M. W. (2003) Targeting the HIV trans-activation responsive region--approaches towards RNA-binding drugs. *ChemBioChem 4*, 972–978.
43. Wang, Y., Hamasaki, K., and Rando, R. R. (1997) Specificity of aminoglycoside binding to RNA constructs derived from the 16S rRNA decoding region and the HIV-RRE activator region. *Biochemistry 36*, 768–779.
44. Werstuck, G., Zapp, M. L., and Green, M. R. (1996) A non-canonical base pair within the human immunodeficiency virus rev-responsive element is involved in both Rev and small molecule recognition. *Chem. Biol. 3*, 129–137.
45. Zapp, M. L., Stern, S., and Green, M. R. (1993) Small molecules that selectively block RNA binding of HIV-1 Rev protein inhibit Rev function and viral production. *Cell 74*, 969–978.
46. von Ahsen, U., Davies, J., and Schroeder, R. (1991) Antibiotic inhibition of group I ribozyme function. *Nature 353*, 368–370.
47. Liu, Y., Tidwell, R. R., and Leibowitz, M. J. (1994) Inhibition of in vitro splicing of a group I intron of *Pneumocystis carinii*. *J. Eukaryot. Microbiol. 41*, 31–38.
48. von Ahsen, U., Davies, J., and Schroeder, R. (1992) Non-competitive inhibition of group I intron RNA self-splicing by aminoglycoside antibiotics. *J. Mol. Biol. 226*, 935–941.
49. Michael, K., Wang, H., and Tor, Y. (1999) Enhanced RNA binding of dimerized aminoglycosides. *Bioorg. Med. Chem. 7*, 1361–1371.
50. Hoch, I., Berens, C., Westhof, E., and Schroeder, R. (1998) Antibiotic inhibition of RNA catalysis: Neomycin B binds to the catalytic core of the td group I intron displacing essential metal ions. *J. Mol. Biol. 282*, 557–569.
51. Tor, Y., Hermann, T., and Westhof, E. (1998) Deciphering RNA recognition: Aminoglycoside binding to the hammerhead ribozyme. *Chem. Biol. 5*, R277–283.
52. Chia, J. S., Wu, H. L., Wang, H. W., Chen, D. S., and Chen, P. J. (1997) Inhibition of hepatitis delta virus genomic ribozyme self-cleavage by aminoglycosides. *J. Biomed. Sci. 4*, 208–216.
53. Mikkelsen, N. E., Brannvall, M., Virtanen, A., and Kirsebom, L. A. (1999) Inhibition of RNase P RNA cleavage by aminoglycosides. *Proc. Natl. Acad. Sci. U.S.A. 96*, 6155–6160.
54. Schroeder, R., Waldsich, C., and Wank, H. (2000) Modulation of RNA function by aminoglycoside antibiotics. *EMBO J 19*, 1–9.
55. Werstuck, G., and Green, M. R. (1998) Controlling gene expression in living cells through small molecule-RNA interactions. *Science 282*, 296–298.
56. Kwon, M., Chun, S. M., Jeong, S., and Yu, J. (2001) In vitro selection of RNA against kanamycin B. *Mol. Cells 11*, 303–311.
57. Jiang, L., Majumdar, A., Hu, W., Jaishree, T. J., Xu, W., and Patel, D. J. (1999) Saccharide-RNA recognition in a complex formed between neomycin B and an RNA aptamer. *Structure 7*, 817–827.
58. Jiang, L., and Patel, D. J. (1998) Solution structure of the tobramycin-RNA aptamer complex. *Nat. Struct. Biol. 5*, 769–774.
59. Francois, B., Russell, R. J., Murray, J. B., Aboul-ela, F., Masquida, B., Vicens, Q., and Westhof, E. (2005) Crystal structures of complexes between aminoglycosides and decoding A-site oligonucleotides: Role of the number of rings and positive charges in the specific binding leading to miscoding. *Nucleic Acids Res. 33*, 5677–5690.
60. Ennifar, E., Paillart, J. C., Bodlenner, A., Walter, P., Weibel, J. M., Aubertin, A. M., Pale, P., Dumas, P., and Marquet, R. (2006) Targeting the dimerization initiation site of HIV-1 RNA with aminoglycosides: From crystal to cell. *Nucleic Acids Res. 34*, 2328–2339.
61. Ennifar, E., Paillart, J. C., Marquet, R., Ehresmann, B., Ehresmann, C., Dumas, P., and Walter, P. (2003) HIV-1 RNA dimerization initiation site is structurally similar to the ribosomal A-site and binds aminoglycoside antibiotics. *J. Biol. Chem. 278*, 2723–2730.

BI8012615